LASER PARTICLE ACCELERATION TECHNOLOGIES: PROBE LASER BEAM DIAGNOSTICS OF EXTENDED PLASMAS

Miklós Á. Kedves, Márk Aladi, József S. Bakos, Gábor Demeter, Gagik Djotyan, Péter Ignácz, Béla Ráczkevi, Zsuzsa Sörlei, János Szigeti

Wigner Research Centre for Physics
Konkoly-Thege Miklós út 29-33, H-1121 Budapest, Hungary

DOI: https://doi.org/10.14232/kvantumelektronika.9.17

Abstract

As plasma-based particle acceleration techniques are becoming intensely developed, the diagnostic tools for the study of the generation and properties of plasmas are increasingly important. We present results on the investigation of probe laser beam diagnostics for the measurement of the plasma density in extended spatial regions. Such extended plasmas are used in particle driven plasma wakefield acceleration experiments for the acceleration of electron/positron bunches to as high as TeV energies in the foreseeable future.

1 Introduction

Novel particle acceleration schemes based on plasma media have been under intense studies for some decades since the introduction of the concept of plasma wakefield acceleration [1]. Practical realization was made possible by the advent of chirped pulse amplification of ultrashort laser pulses resulting in multiterawatt intensities in a pulse [2]. Beside the laser particle acceleration technique other schemes have also been pursued utilizing the enormous electric fields generated by the charge separation in the plasma. One of the very promising projects is the Advanced Proton Driven Plasma Wakefield Acceleration Experiment (AWAKE) at CERN which utilizes the energetic proton beams from the Super Proton Synchrotron (SPS) for the acceleration of electron bunches in a plasma medium [3,4]. These methods are especially attractive because of the huge accelerating potential that can be several orders of magnitude higher than in conventional accelerators, making it feasible to construct compact accelerators of significantly smaller size and cost. The AWAKE group demonstrated the acceleration of witness electron bunches to 2 GeV in 2018 [5].

Instead of the multi-km long structures, the AWAKE device incorporates a 10 m long plasma chamber where acceleration actually takes place. However, because of the strict requirements for plasma uniformity, this plasma is enclosed in the completely closed vessel where hardly any access can be open for plasma diagnostics. Our group is working on the development of different diagnostic techniques to characterize the plasma generated in extended spatial regions. We have constructed an experimental arrangement containing a 75 cm long rubidium vapor cell where plasma can be generated by a Ti-sapphire laser pulse, and optical observations can be carried out either longitudinally or in transverse directions at several locations along the plasma column.

The study of the propagation of intense ultrashort laser pulses in a medium and its nonlinear effects (self-focusing, filamentation) is very interesting and important in itself, and has been carried out for several decades [6]. However, very little is known about the special case when the ionizing laser pulse is resonant with a single-photon transition from the ground state of the gaseous target material. In the particular experiments of the AWAKE project and also our investigations rubidium vapor is used for generating the plasma with the pulses of a Ti-sapphire laser, which is in direct resonance with

the Rb atom. Therefore, our group is also engaged in developing theoretical models and computer simulations for the better understanding of these nonlinear pulse propagation phenomena [7]. In this paper some of the results and observations of our probe beam absorption experiments and computer simulations are summarized.

2 Experimental arrangement

The extended plasma column is generated in a 75 cm long glass cell filled with rubidium atomic vapor by the intense pulses of a Ti-sapphire laser system (Coherent Hidra). Rubidium is used as the target material because of its low first and high second ionization potential, which enables a robust single photoionization process. The glass cell is heated by an oven, placed in a vacuum chamber for good heat insulation. Maximum rubidium atomic density of about $10^{15}\mathrm{cm}^{-3}$ can be generated this way. The vapor is irradiated by the laser pulses in the longitudinal direction with the unfocused beam of the Hidra system. The maximum pulse energy of the laser is 30 mJ, the pulse duration is 40 fs, and the beam diameter is about 12 mm. However, in order to avoid self-focusing of these intense pulses in air, lower pulse energies of up to 15 mJ were used, and the pulse length was increased to about 300 fs by varying the pulse compression in the grating compressor of the laser. This resulted in maximum pulse intensities around $10^{11}\mathrm{W}/\mathrm{cm}^2$ and frequency-swept (chirped) pulses rather than transform limited ones.

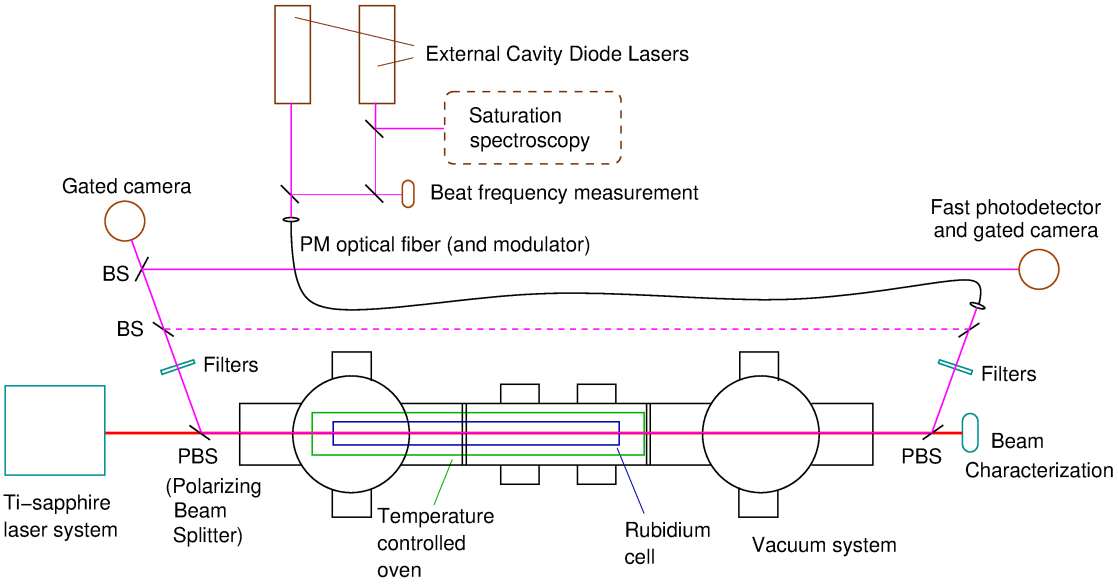

Figure 1: *Experimental arrangement of the longitudinal probe beam diagnostic measurement on Rb plasma.*

The ionization fraction of the rubidium vapor was determined by measuring the absorption of a near-resonant probe laser beam transmitted through the plasma column in the longitudinal direction opposite to the propagation of the ionizing laser pulse. The probe laser is an external cavity diode laser (ECDL; New Focus TLB-6712) detuned from the atomic resonance line of rubidium by several GHz. The frequency of the probe laser was continuously monitored by detecting its beat frequency with another ECDL that was stabilized to an atomic transition. The attenuation of the probe laser beam was measured either by a fast (4.5 GHz) photodiode (New Focus 1591) or gated and intensified cameras with sub-microsecond exposure times. In some series of experiments a Mach-Zehnder interferometer arrangement was formed by inserting a reference probe laser path, and the interference of the two beams was registered. Transverse absorption measurements have also been carried out, but these are not treated here.

The details of the determination of the ionization fraction will be published in a separate paper. Briefly, the transmitted power of the probe laser was measured in plasma (P_{plas}) and in atomic vapor

(P_{vap}) (i.e. with and without the ionizing pulse), and also in vacuum (more precisely, in the residual vapor at room temperature: P_{res}). Using the relative transmission ratios the ionization fraction can be calculated from the following formula:

$$\rho = \frac{\ln\left(\frac{P_{plas}}{P_{vap}}\right)}{\ln\left(\frac{P_{res}}{P_{vap}}\right)}.$$

At the maximum ionizing pulse intensity of $10^{11} W/cm^2$ with negative frequency chirp, a maximum ionization fraction of about 40% was obtained. In our earlier experiments with 2 mJ, 40 fs pulses the interference signal of the probe laser beams was analyzed, and ionization fraction values around 10% were obtained [8].

3 Discussion of the experimental observations

3.1 Focusing/defocusing of the probe laser beam

In our first series of experiments we used a fiber-coupled fast photodetector for the detection of the transmitted probe beam power with high temporal resolution. Since the absorption measurement can detect the density of the (ground state) atomic species in the cell, the transmitted power is expected to increase after the ionizing laser pulse. However, we observed serious decrease in the measured signal. This unexpected behaviour was explained by the assumption that the probe beam was defocused by the radial variation of the refractive index in the plasma column, forming a lens in the middle of the laser beam path. This would then focus the probe laser beam depending on the laser frequency and the density distribution of the residual atomic species.

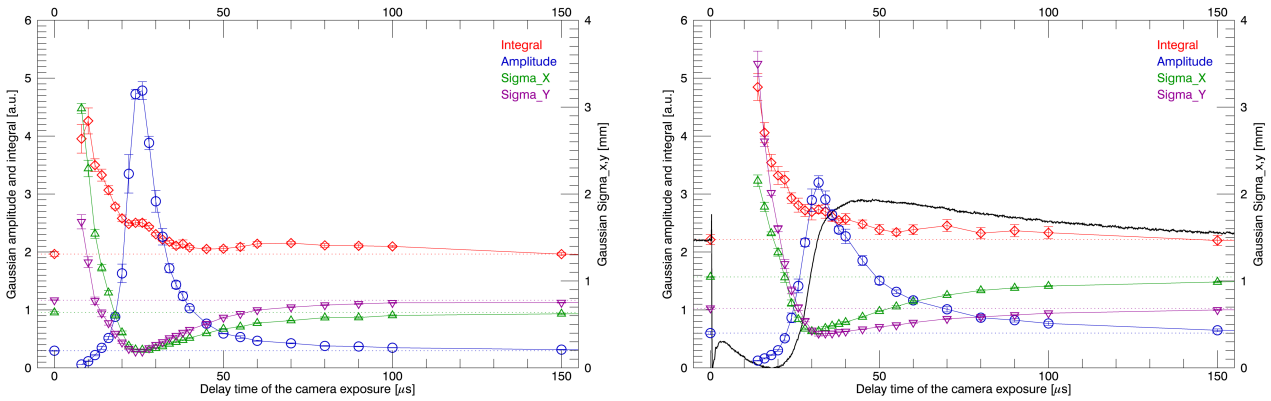

(a) *Camera closer to the plasma cell* (b) *Camera farther from the plasma cell*

Figure 2: *The dependence of the Gaussian beam parameters on the delay time of the camera exposure. The black line in (b) shows the signal of the fast photodiode at the same location.*

In order to check this assumption the transmitted probe beam was detected with gated cameras at two different distances from the plasma column. The probe laser frequency was tuned above the rubidium resonance lines by 4 GHz. The recorded images were evaluated by fitting 2-dimensional Gaussian-distributions to the data. The transmitted beam power can be characterized by the integral of the obtained Gaussian distribution, which is proportional to the product of the amplitude and the σ_x and σ_y width parameters: $I = 2\pi Amp \cdot \sigma_x \sigma_y$. In the first few microseconds after plasma creation the probe beam is strongly blown up and scattered out of the camera sensor area, therefore no data can be evaluated in this delay region. The results of the fitting procedure can be seen in Figure 2, where the decrease in the Gaussian sigma parameters indicates the focusing of the probe beam. At

zero delay time the probe beam parameters without ionizing laser pulse are depicted, and the dotted lines represent the level to which the values return with plasma relaxation. It can also be seen that the minimum beam size is observed at a longer delay setting on the camera farther from the plasma, that is, the focal distance of the relaxing plasma column is getting longer with time after the ionization.

The integral of the calculated Gaussian distribution characterizes the transmitted probe laser beam power, and the ionization fraction can be calculated from the increase of this value in the plasma with respect to the vapor. In Figure 2b the continuous black line shows the signal of the fast photodetector that was placed close to the location of the second camera. It can be clearly seen that the photodetector signal cannot represent the transmitted probe laser power as the beam is defocused and the coupling into the detector fiber is strongly reduced.

Figure 3 shows the obtained beam spot sizes at different probe laser detuning directions. In the case of a positive detuning (+4 GHz from the uppermost hyperfine level of the rubidium atom), the refractive index of the atomic vapor is below one, and the refractive index of the plasma is very close to unity. Therefore, the refractive index is higher in the middle of the plasma column, and a positive lens is formed. This focuses the probe laser beam with a short focal length at the beginning of the plasma relaxation, and then the focal point is shifted farther away. In the case of negative detunings (-4 GHz from the lowermost hyperfine level), however, a negative lens is created, and the probe beam is defocused all the way along the plasma relaxation. The lens formed in the extended spatial region can be described as a Graded Index (GRIN) lens. Plasma-based GRIN lenses have also been observed to generate a ring-shaped beam distribution after propagation in the medium [9].

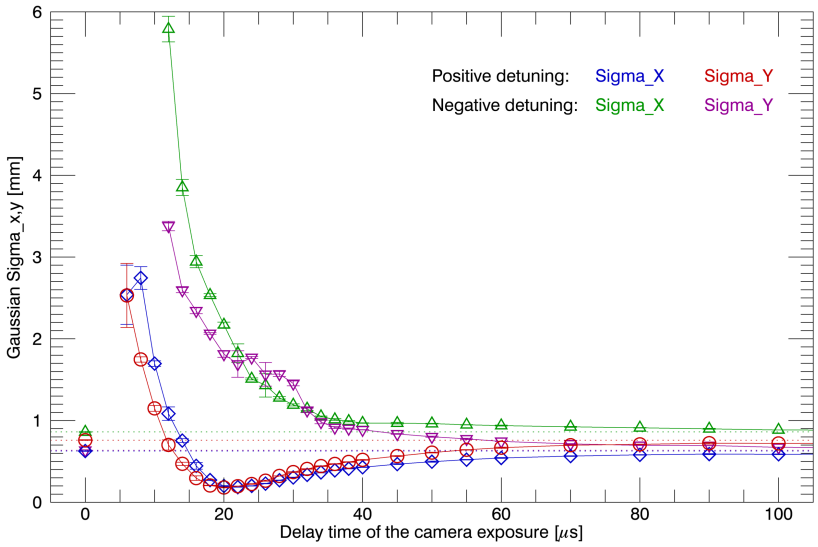

Figure 3: *Dependence of the transmitted probe beam spot sizes on the exposure delay at positive and negative detuning values.*

3.2 Effect of the chirp direction of the ionizing laser

Since we were working with chirped pulses for the creation of the plasma, we have also examined the dependence of the ionization efficiency of the laser pulse on the direction of the frequency sweep. In Figure 4 different diagnostic signals can be seen which were measured with different chirp directions with a positive probe laser beam detuning. In the case of negative frequency chirp, the interference signal detected by the fast photodiode shows more oscillations indicating a larger phase shift, which also corresponds to a bigger density variation [8]. The Gaussian integral and spot size parameters measured with the gated camera also display a more intense ionization effect. Although the ionization fraction cannot be easily deduced from these data for the series with positive chirp, it can clearly be

seen that there is a marked difference between the two cases, and the effect of the ionizing laser pulse on the rubidium vapor in the case of the negative chirp is much more pronounced, suggesting that the ionization efficiency is also higher. In order to study this dependence systematically we are planning measurements of the frequency evolution of the ionizing laser pulse using a Frequency Resolved Optical Gating (FROG) instrument.

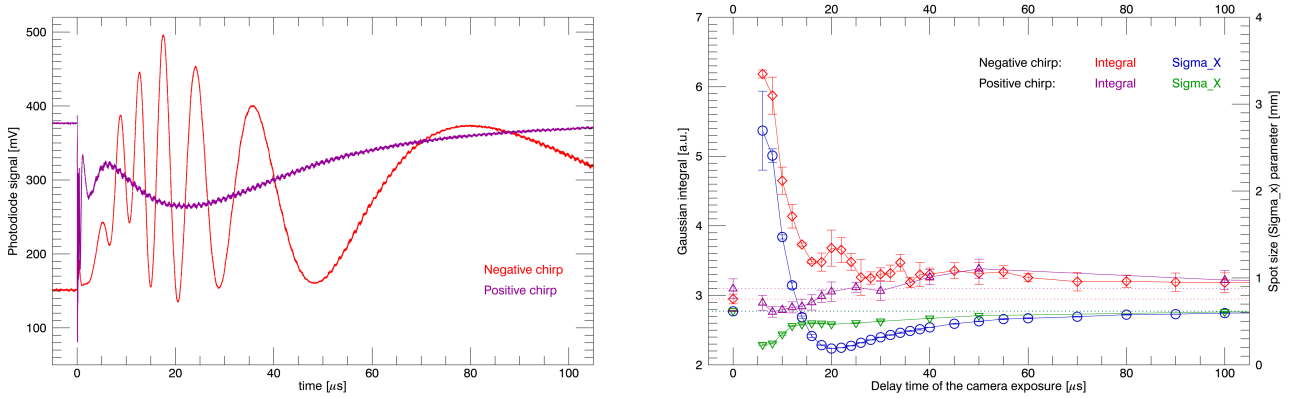

(a) *Interference signal on the photodiode* (b) *Gaussian integral and spot size parameters*

Figure 4: *Interference signal (a) and Gaussian integral and spot size parameters (b) for different chirp directions of the ionizing laser pulse.*

4 Simulation of the propagation of resonant ionizing laser pulses

A theoretical model was developed to describe the propagation of ionizing, resonant laser pulses in rubidium vapor. The model follows the concept of [7], but the atomic model is more complex, utilizing 10 atomic bound state levels. Atomic polarization is calculated from the time-dependent probability amplitudes of the Schrödinger equation and a first order propagation equation is written for the envelope of the laser pulse in frequency space. Ionization is included as a set of phenomenological loss terms in the Schrödinger equation. Calculations show that the laser pulse experiences strong self-focusing in the nonlinear medium and given sufficient energy, a plasma channel with very close to 100 % ionization is formed.

5 Summary

Diagnostic methods for the measurement of the parameters of extended plasma columns are being developed. The plasma density is determined using longitudinal probe laser absorption where the focusing and defocusing of the probe laser beam was observed. It should be noted that the plasma was not completely ionized in our case, and therefore the radial distribution of the residual atomic vapor acts as a lens. The same diagnostics have also been used in the AWAKE experimental apparatus, where the ionization of the gas can be complete due to the significantly higher laser intensity. Therefore much less significant focusing effects were observed there. The data are under evaluation and will be published soon, and also further development work of the method is being carried out.

The ionization efficiency of the frequency chirped laser pulses was observed to depend on the direction of the frequency sweep of the ionizing laser. The efficiency was higher for negatively chirped laser pulses. In order to study this effect the systematic measurement of the frequency chirp of the ionizing laser pulse is necessary. In the following a series of experiments is planned using a FROG instrument for the precise determination of the spectral phase characteristics of the chirped laser pulses.

A relatively simple theoretical model has been developed for computing the response of the medium in the presence of strong resonant nonlinearity and ionization. A marked difference has been found in comparison with the nonresonant filamentation processes.

6 Acknowledgments

We would like to thank Joshua T. Moody, Patric Muggli and the AWAKE team for the fruitful collaboration. The support to our research project from the NKFIH under the programme "NEMZETKÖZI KUTATÁSI INFRASTRUKTÚRÁK KIHASZNÁLTSÁGÁNAK TÁMOGATÁSA 2019-2.1.6-NEMZ _KI-2019-00004", as well as from Péter Lévai is gratefully acknowledged.

7 References

[1] T. Tajima and J. M. Dawson, Phys. Rev. Lett. **43**, 267 (1979).
https://doi.org/10.1103/PhysRevLett.43.267

[2] P. Maine, D. Strickland, P. Bado, M. Pessot and G. Mourou, IEEE J. Quantum Electron, A **24**, 398 (1988).
https://doi.org/10.1109/3.137

[3] A. Caldwell et al., Nulc. Instr. Methods A **829**, 3 (2016).
https://doi.org/10.1016/j.nima.2015.12.050

[4] E. Gschwendtner et al., Nulc. Instr. Methods A **829**, 76 (2016).
https://doi.org/10.1016/j.nima.2016.02.026

[5] E. Adli et al., Nature **561**, 363 (2018).
https://doi.org/10.1038/s41586-018-0485-4

[6] A. Couairon and A. Mysyrowicz, Physics Reports **441**, 47 (2007).
https://doi.org/10.1016/j.physrep.2006.12.005

[7] G. Demeter, Phys. Rev. A **99**, 063423 (2019).
https://doi.org/10.1103/PhysRevA.99.063423

[8] G. P. Djotyan et al., Nucl. Instr. Methods A **884**, 25 (2018).
https://doi.org/10.1016/j.nima.2017.12.004

[9] Chao Tan et al. J. Opt. **15** 125202 (2013).
https://doi.org/10.1088/2040-8978/15/12/125202